

Co-Learning with Pre-Trained Networks Improves Source-Free Domain Adaptation

Wenyu Zhang, Li Shen
Institute for Infocomm Research, A*STAR

Chuan-Sheng Foo
Institute for Infocomm Research, A*STAR
Centre for Frontier AI Research, A*STAR

Abstract

Source-free domain adaptation aims to adapt a source model trained on fully-labeled source domain data to a target domain with unlabeled target domain data. Source data is assumed inaccessible due to proprietary or privacy reasons. Existing works use the source model to pseudolabel target data, but the pseudolabels are unreliable due to data distribution shift between source and target domain. In this work, we propose to leverage an ImageNet pre-trained feature extractor in a new co-learning framework to improve target pseudolabel quality for finetuning the source model. Benefits of the ImageNet feature extractor include that it is not source-biased and it provides an alternate view of features and classification decisions different from the source model. Such pre-trained feature extractors are also publicly available, which allows us to readily leverage modern network architectures that have strong representation learning ability. After co-learning, we sharpen predictions of non-pseudolabeled samples by entropy minimization. Evaluation on 3 benchmark datasets show that our proposed method can outperform existing source-free domain adaptation methods, as well as unsupervised domain adaptation methods which assume joint access to source and target data.

Domain adaptation (DA) aims to tackle the domain shift problem by transferring knowledge from a fully-labeled source domain to an unlabeled target domain. The classic setting of *unsupervised domain adaptation* assumes source and target data are jointly available for training [41]. Motivated by the theoretical bound on target risk derived in [4], a key strategy is to minimize the discrepancy between source and target features to learn domain-invariant features [10, 11, 13, 15, 22, 25, 38, 43, 47]. However, access to source data can be impractical due to data privacy concerns. Recently, the *source-free domain adaptation* setting is proposed [26] to split training into two processes: (a) training network with fully labeled source data, and (b) adapting source model with unlabeled target data. An example use case in a corporate context is when the vendor organization has a labeled source dataset for training a source model, and potential clients who are interested in the same task and need a model suitable for their own target environments, but data sharing for joint training cannot be achieved due to proprietary or privacy reasons. The vendor organization makes available the source model, which the clients can adapt with their target data and any other resources available. In this work, we assume the role of clients who have received the source model.

We focus on the image classification task where source and target domain share the same label space. The source model is typically obtained by training a selected network, initialized by ImageNet weights, on source data with supervised loss. For adaptation, existing source-free DA methods generate or estimate source-like representations to align source and target distributions [8, 34], make use of local clustering structures in the target data [44–46], and learn semantics through self-supervised tasks [27, 42]. [21, 23, 26] use the source model to generate target data pseudolabels for finetuning, and [6, 17, 27] further select samples with the low-entropy or low-loss criterion. However, model calibration is known to degrade under data distribution shift [32]. We observe in Figure 1 that target data pseudolabels produced by source model can be biased, and outputs such as prediction confidence (and consequently entropy and loss)

1. Introduction

Deep neural networks have demonstrated remarkable ability in diverse applications, but their performance typically relies on the assumption that training (*source domain*) and test (*target domain*) data distributions are the same. This assumption can be violated in practice when the source data does not fully represent the entire data distribution due to difficulties of real-world data collection. Target samples distributed differently from source samples (due to factors such as background, illumination and style [12, 18]) are subject to *domain shift* (also known as *covariate shift*), and can severely degrade model performance.

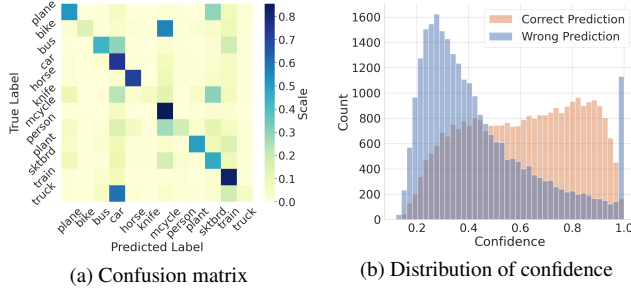


Figure 1. VisDA-C source-trained ResNet-101 produces unreliable pseudolabels on target samples, and is over-confident on a significant number of incorrect predictions.

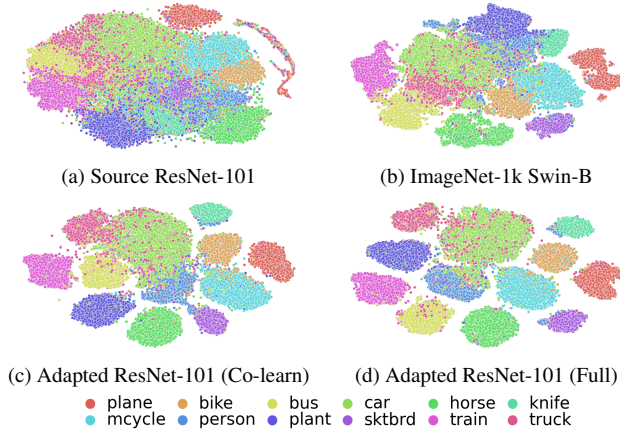


Figure 2. t-SNE visualization of VisDA-C target domain features by source ResNet-101, ImageNet-1k Swin-B and source ResNet-101 adapted by proposed co-learning with ImageNet-1k Swin-B. Features are extracted at the last pooling layer before the classification head. Samples are colored by class.

may not reflect accuracy and cannot reliably be used alone to improve pseudolabel quality.

The source model is limited by the choice of network architecture and training scheme, determined based on factors such as source data quantity, computational resources available, device specifications for model training and eventual deployment, and best practices at the time. New architectures and training schemes are constantly developed on publicly available datasets such as ImageNet, and while it may be unrealistic for the client to repeatedly request the vendor to incorporate new techniques to re-train the source model in the example use case, we seek to answer the question: *Given a source model, whether and how modern pre-trained networks can help its adaptation?*

As compared to source models, we find that ImageNet feature extractors can be more compatible with the target domain. Figure 2 shows VisDA-C target domain features by different feature extractors. Features are extracted at the last pooling layer before the classification head. The source model is initialized with ImageNet-1k weights before training on source domain dataset as in standard practice, and

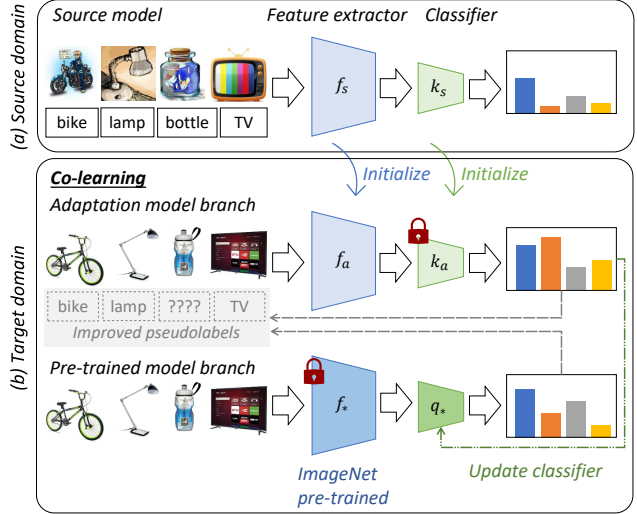


Figure 3. Overview: (a) Source model trained on source domain is provided. (b) For source-data-free adaptation to target domain, we propose to adapt the source model through a co-learning framework where the adaptation model and an ImageNet pre-trained model collectively produce more reliable pseudolabels for finetuning. After co-learning, we sharpen predictions of non-pseudolabeled samples by entropy minimization.

assuming fair access to ImageNet-1k pre-trained weights, we demonstrate with an ImageNet-1k Swin-B feature extractor. Swin [28] is a recent transformer architecture with strong representation learning ability. Even without training on VisDA-C images, the Swin-B feature extractor produces more class-discriminative target domain representations as the target style (real photos) is more similar to ImageNet style than to source style (synthetic images), and the ImageNet weights are not source-biased.

In this paper, we propose to incorporate such a target-compatible feature extractor to help correct source model prediction bias and produce more accurate target pseudolabels to finetune the source model. We design a two-branch co-learning framework where the adaptation and pre-trained model branch iteratively updates, and a pseudolabelling strategy for the two branches to collectively generate more accurate pseudolabels. Finally, predictions for non-pseudolabeled samples are sharpened by entropy minimization. We provide an overview of our proposed method in Figure 3, and summarize our contributions:

- We are the first to explore the usability of publicly available pre-trained networks for source-free DA given a fixed source model;
- We propose a new methodology that uses an ImageNet pre-trained feature extractor to improve target pseudolabel quality for finetuning the source model;
- The proposed method achieves state-of-the-art performance on 3 benchmark image classification datasets

for domain adaptation.

2. Related Works

2.1. Unsupervised domain adaptation

In traditional unsupervised DA, networks are trained jointly on labeled source and unlabeled target dataset to optimize task performance on the target domain [41]. A popular strategy is to learn domain-invariant features via minimizing domain discrepancy measured by an inter-domain distance or adversarial loss [10, 11, 13, 15, 22, 25, 38, 43, 47]. [30] learns a distribution of classifiers to better identify local regions of misalignment between source and target domains, and [7, 31] facilitate alignment between distant domains by generating intermediate domains. [24] augments source data to assume target style. Other methods encourage target representations to be more class-discriminative by learning cluster structure [39] or minimizing uncertainty [14]. Amongst confidence-based methods, [11] trains a spherical neural network to select target samples for pseudolabeling, [9, 31] selects high confidence predictions as positive pseudolabels and [9] applies mean teacher from semi-supervised learning. Due to the assumed access to both source and target data, these methods are unsuitable when source data is not available for joint training.

2.2. Source-free domain adaptation

In source-free DA, the source model is adapted with unlabeled target dataset. [19, 20] train on source domain with auxiliary tasks or augmentations and [36] calibrates uncertainties with source data to obtain improved source models, but these strategies cannot be applied on the client-side where source data is not accessible. Some methods make use of local clustering structures in the target dataset to learn class-discriminative features [44–46], and learn semantics through self-supervised tasks such as rotation prediction [27, 42]. [35] proposes multi-centric clustering, but the cluster number is not straightforward to select for each dataset. [42] learns a new target-compatible classifier, and [23] generates target-style data with a generative adversarial network to improve predictions. Other methods generate source-like representations [34] or estimate source feature distribution to align source and target domains [8]. [21, 23, 26] use the source model to generate pseudolabels for the target dataset, and align target samples to the source hypothesis through entropy minimization and information maximization. To improve pseudolabel quality, [6, 17, 27] select target samples with low entropy or loss for pseudolabeling and finetuning the source model. We find that source model outputs may not reliably reflect target pseudolabel accuracy due to domain shift in Figure 1. We instead make use of an ImageNet pre-trained feature extractor to correct the source bias and produce more reliable pseudolabels.

3. Proposed Method

Provided with the source model, our goal is to adapt it with unlabeled target data. The source model can produce unreliable target pseudolabels due to domain shift, and we propose to leverage publicly available ImageNet feature extractors to generate improved pseudolabels to finetune the source model. We introduce notations and motivation in Section 3.1, resources for pre-trained feature extractors in Section 3.2 and the proposed source-free DA method in Section 3.3.

3.1. Preliminaries

We denote the source and target distributions as \mathcal{P}_s and \mathcal{P}_t , and observations as $\mathcal{D}_s = \{(x_s^n, y_s^n)\}_{n=1}^{N_s}$ and $\mathcal{D}_t = \{(x_t^n, y_t^n)\}_{n=1}^{N_t}$, for image $x \in \mathcal{X}$ and one-hot classification label $y \in \mathcal{Y}$. The two domains share the same label space $\mathcal{Y}_s = \mathcal{Y}_t$ with $|\mathcal{Y}| = L$ classes, but have different data space $\mathcal{X}_s \neq \mathcal{X}_t$. In the source-free DA setting, source data \mathcal{D}_s and target labels $\{y_t^n\}_{n=1}^{N_t}$ are not accessible during adaptation. Knowledge on source data is captured by a source model.

The source model trained on \mathcal{D}_s is composed of feature extractor f_s parameterized by Θ_s that yields learned representations $z_s = f_s(x; \Theta_s)$, and classifier k_s parameterized by Ψ_s that yields logits $g_s = k_s(z_s; \Psi_s)$. Estimated class probabilities are obtained by $p_s = \sigma(g_s)$ for softmax function σ where $p_s[i] = \frac{\exp(g_s[i])}{\sum_{j=1}^L \exp(g_s[j])}$ for class i , and the predicted class is $\hat{y}_s = \arg \max_i p_s[i]$.

For a hypothesis $h \in \mathcal{H}$, we refer to $\epsilon_t(h, \ell_t) = E_{x \sim P_t} \epsilon(h(x), \ell_t(x))$ as the target risk of h with respect to the true target labeling function ℓ_t . To understand the relationship of h and ℓ_t with the source model, we assume an error function ϵ such as $\epsilon(v, v') = |v - v'|^\alpha$ that satisfies triangle equality following [4, 5], then

$$\epsilon_t(h, \ell_t) \leq \epsilon_t(h, h_p) + \epsilon_t(h_p, \ell_t) \quad (1)$$

where h_p is a pseudolabeling function, such as hypothesis $k_s \circ f_s$ learned on source data. The second term $\epsilon_t(h_p, \ell_t)$ is target pseudolabeling error by h_p , and the first term is minimized by $h = h_p$. Motivated by the bound in Equation 1, we propose an iterative approach to improve the pseudolabeling function h_p and to finetune h towards h_p .

3.2. Pre-trained feature extractor

As the source model may be biased towards the source data distribution after training on it, we propose leveraging an ImageNet feature extractor f_* parameterized by Θ_* that is more compatible with the target domain in producing more class-discriminative representations. This feature extractor is used to improve target pseudolabels, further explained in Section 3.3.

Resources: Open-source libraries and platforms such as Torch [2], TensorFlow [3] and Hugging Face [1] are

$\hat{y}_a = \hat{y}_*$	$\text{Conf}(\hat{y}_a) > \gamma$	$\text{Conf}(\hat{y}_*) > \gamma$	Pseudolabel \tilde{y}
✓	✓/✗	✓/✗	\hat{y}_a
✗	✓	✓	-
✗	✓	✗	\hat{y}_a
✗	✗	✓	\hat{y}_*
✗	✗	✗	-

Table 1. MatchOrConf pseudolabeling strategy with adaptation and pre-trained model predictions, \hat{y}_a and \hat{y}_* , and confidence threshold γ . Dash (-) means that sample is not pseudolabeled.

straightforward resources for pre-trained networks. In our experiments, we utilize feature extractors pre-trained on ImageNet-1k to match the use of ImageNet-1k networks in training source models. These ImageNet feature extractors may be more target-compatible than the source feature extractor because (1) the larger ImageNet dataset is not source-biased and may better represent the data distribution, (2) modern state-of-the-art network architectures can learn better representations. As the client in the example use case in Section 1, without having to request and wait for the vendor to update the source model, the client can leverage the latest pre-trained networks for adaptation.

3.3. Source-free domain adaptation

We propose a co-learning framework to progressively adapt the source model $\{f_s, k_s\}$ with the ImageNet pre-trained feature extractor f_* . The framework consists of two branches: (1) adaptation model branch $\{f_a, k_a\}$ initialized by source model $\{f_s, k_s\}$, (2) pre-trained model branch initialized by f_* and a newly-estimated task classifier q_* . Inspired by [26] on their use of weights in the nearest-centroid-classifier (NCC), we construct q_* as a weighted nearest-centroid-classifier where the centroid μ_i for class i is the sum of f_* features, weighted by estimated class probabilities of the adaptation model:

$$\mu_i = \frac{\sum_x \sigma(k_a(f_a(x; \Theta_a); \Psi_a))[i] f_*(x; \Theta_*) / \|f_*(x; \Theta_*)\|}{\sum_x \sigma(k_a(f_a(x; \Theta_a); \Psi_a))[i]} \quad (2)$$

$$g_*[i] = q_*(f_*(x; \Theta_*))[i] = \frac{f_*(x; \Theta_*) \cdot \mu_i}{\|f_*(x; \Theta_*)\| \|\mu_i\|} \quad (3)$$

$$p_* = \sigma(g_*/\text{Temperature}) \quad (4)$$

The weighted NCC leverages the target domain class-discriminative cluster structures in f_* features. In Equation 4, predictions p_* are sharpened with $\text{Temperature} = 0.01$ since the logits g_* calculated through cosine similarity are bounded in $[-1, 1]$.

Co-learning: We alternate updates on the adaptation and pre-trained model branch as each adapts to the target domain and produces more accurate predictions to improve the other branch. Each round of update on the two branches is referred to as a co-learning episode. For the adaptation

Algorithm 1 Proposed source-free DA

Input: Target images $\{x_t^n\}_{n=1}^{N_t}$; source model $k_s \circ f_s$ parameterized by (Θ_s, Ψ_s) ; pre-trained feature extractor f_* parameterized by Θ_* ; confidence threshold γ ; learning rate η ; # episodes I ;

- 1: **procedure** CO-LEARNING
- 2: Initialize weights of adaption model branch $k_a \circ f_a$ by $(\Theta_a, \Psi_a) \leftarrow (\Theta_s, \Psi_s)$
- 3: Initialize pre-trained model branch classifier q_* by computing centroids according to Equation 2
- 4: **for** episode $i = 1 : I$ **do**
- 5: Construct pseudolabel dataset \tilde{D}_t by MatchOrConf strategy with threshold γ in Table 1
- 6: Compute loss $L_{co-learn}(\Theta_a)$ in Equation 5
- 7: Update weights $\Theta_a \leftarrow \Theta_a - \eta \nabla L_{co-learn}(\Theta_a)$
- 8: Update centroids in q_* according to Equation 2
- 9: **end for**
- 10: **end procedure**
- 11: **procedure** PREDICTION SHARPENING
- 12: Construct pseudolabel dataset \tilde{D}_t by MatchOrConf strategy with threshold γ in Table 1
- 13: **for** episode $i = 1 : I$ **do**
- 14: Compute loss $L_{sharpen}(\Theta_a)$ in Equation 6
- 15: Update weights $\Theta_a \leftarrow \Theta_a - \eta \nabla L_{sharpen}(\Theta_a)$
- 16: **end for**
- 17: **end procedure**
- 18: **return** Adaptation model $k_a \circ f_a$ with weights (Θ_a, Ψ_a)

model branch, we freeze classifier k_a and update feature extractor f_a to correct its initial bias towards the source domain. We finetune f_a with cross-entropy loss on improved pseudolabeled samples, further described in the next paragraph. For the pre-trained model branch, we freeze feature extractor f_* to retain the target-compatible features and update classifier q_* . The centroids are updated by Equation 2 using estimated class probabilities $\sigma(k_a(f_a(x; \Theta_a); \Psi_a))$ of the current adaptation model. Improvements in the adaptation model predictions each episode give more accurate class centroids in the pre-trained model branch.

Improved pseudolabels: We improve pseudolabels each episode by combining predictions from the two branches using the MatchOrConf strategy in Table 1. Denoting \hat{y}_a and \hat{y}_* as the adaptation and pre-trained model predictions, respectively, the pseudolabel \tilde{y} given is $\hat{y}_a (= \hat{y}_*)$ if the predicted classes match, and the predicted class with higher confidence level otherwise. Confidence level is determined by a threshold γ . Remaining samples are not pseudolabeled. The co-learning objective function for the adaptation model is

$$L_{co-learn}(\Theta_a) = - \sum_{(x, \tilde{y}) \in \tilde{D}_t} \tilde{y} \cdot \log(p_a) \quad (5)$$

where $p_a = \sigma(k_a(f_a(x; \Theta_a); \Psi_a))$ and \tilde{D}_t is the pseudolabeled target dataset.

Prediction sharpening: After co-learning, the pre-trained model branch is discarded. We further sharpen the adaptation model predictions for non-pseudolabeled samples by entropy minimization:

$$L_{sharpen}(\Theta_a) = - \sum_{(x, \tilde{y}) \in \tilde{D}_t} \tilde{y} \cdot \log(p_a) - \sum_{x \in D_t \setminus \tilde{D}_t} p_a \cdot \log(p_a) \quad (6)$$

Algorithm 1 summarizes the source-free DA method.

4. Experiments and Results

We evaluate on 3 benchmark image classification datasets for domain adaptation. We describe experimental setups in Section 4.1 and results in Section 4.2.

4.1. Experimental setups

Datasets. **Office-31** [37] has 31 categories of office objects in 3 domains: Amazon (A), Webcam (W) and DSLR (D). **Office-Home** [40] is a challenging dataset with 65 categories of everyday objects in 4 domains: Art (A), Clipart (C), Product (P) and Real World (R). **VisDA-C** [33] is a popular 12-class dataset for evaluating synthetic-to-real shift, with synthetic rendering of 3D models in source domain and Microsoft COCO real images in target domain.

Evaluation. We compare adaptation performance with a range of unsupervised and source-free domain adaptation methods, described in Section 2. We report classification accuracy on the target domain for all domain pairs in Office-31 and Office-Home, and average per-class accuracy on the real domain in VisDA-C.

Implementation details. We follow the network architecture and training scheme in [26, 27] to train source models: Office-31 and Office-Home use ResNet-50 and VisDA-C uses ResNet-101 initialized with ImageNet-1k weights for feature extractor plus a 2-layer linear classifier with weight normalization, trained on labeled source data with supervised loss. For our proposed source-free domain adaptation approach, we experiment with the following ImageNet-1k feature extractors for co-learning: ResNet-50, ResNet-101, ConvNeXt-S, Swin-S, ConvNeXt-B and Swin-B, where S and B denote the small and base versions of the architectures, respectively. This list is not exhaustive and is meant as a demonstration that state-of-the-art networks can be successfully plugged into our proposed framework. ConvNeXt convolutional networks [29] and Swin transformers [28] are recently-released architectures for computer vision tasks that demonstrated improved robustness to domain shifts [16]. In the training procedure, we train using SGD optimizer for 15 episodes each for co-learning and prediction sharpening, with batch size 50 and learning

rate 0.01 decayed to 0.001 after 10 episodes. We set confidence threshold $\gamma = 0.5$ for Office-31 and Office-Home and $\gamma = 0.1$ for VisDA-C, with further analysis in Section 5.

4.2. Results

In Table 2 for Office-31, our method achieves the highest accuracy of 93.6% averaged across six source-target domain pairs when ImageNet-1k Swin-B feature extractor is used in the pre-trained model branch. Amongst the feature extractors tested for co-learning, ConvNeXt-B and Swin-B generally result in the highest accuracy, followed by ConvNeXt-S and Swin-S, and finally ResNet-50 and ResNet-101. Even by using ImageNet-1k ResNet-50, the same architecture as source model, classification accuracy increases by 9.1% over the original source model accuracy.

In Table 3 for Office-Home, our adapted model co-learned with ImageNet-1k Swin-B obtains the highest accuracy for each source-target domain pair, and has an average accuracy 83.6% which is 10.6% higher than the best existing method SHOT++ (73.0%). Powerful pre-trained networks can have class-discriminative features applicable to target domain, and the large performance boost reflects the advantage of using them to adapt the source models.

In Table 4 for VisDA-C, the highest average per-class accuracy is again attained by our adapted model (88.4%) co-learned with ImageNet-1k Swin-B. In fact, on this dataset, ImageNet style overlaps with the realistic target style, such that even a smaller ImageNet-1k ResNet-50 is more target-compatible than the source ResNet-101 trained on synthetic source domain. Co-learning with ImageNet-1k ResNet-50 already results in a classification accuracy of 83.7%, which is higher than recent source-free DA methods SFDA, 3C-GAN and SHOT, and significantly improves over the source model by 37.8%.

5. Further Analysis

We conduct further experiments to analyze the co-learning and prediction sharpening procedures in Section 5.1 and 5.2, and discuss considerations on the feature extractor in the pre-trained model branch in Section 5.3.

5.1. Co-learning

We fix the pre-trained model branch to use ImageNet-1k ConvNeXt-S feature extractor to focus on analyzing the domain adaptation process during co-learning.

Pre-trained model branch. We experiment on the pre-trained model branch with a subset of domain pairs from Office-Home dataset in Table 5. We choose to update no component or different component(s) of the pre-trained network, such as feature extractor, weighted nearest-centroid-classifier (NCC) and a linear 1-layer logit projection layer inserted after NCC. Finetuning just the classifier achieves

Method	Office-31						
	A \rightarrow D	A \rightarrow W	D \rightarrow A	D \rightarrow W	W \rightarrow A	W \rightarrow D	Avg
MDD [47]	93.5	94.5	74.6	98.4	72.2	100.0	88.9
GVB-GD [7]	95.0	94.8	73.4	98.7	73.7	100.0	89.3
MCC [14]	95.6	95.4	72.6	98.6	73.9	100.0	89.4
GSDA [13]	94.8	95.7	73.5	<u>99.1</u>	74.9	100.0	89.7
CAN [15]	95.0	94.5	78.0	<u>99.1</u>	77.0	99.8	90.6
SRDC [39]	95.8	95.7	76.7	77.1	100.0	100.0	90.8
SFDA [17]	92.2	91.1	71.0	98.2	71.2	99.5	87.2
SHOT [26]	94.0	90.1	74.7	98.4	74.3	<u>99.9</u>	88.6
SHOT++ [27]	94.3	90.4	76.2	98.7	75.8	<u>99.9</u>	89.2
3C-GAN [23]	92.7	93.7	75.3	98.5	77.8	99.8	89.6
AaD [46]	96.4	92.1	75.0	<u>99.1</u>	76.5	100.0	89.9
A ² Net [42]	94.5	94.0	76.7	99.2	76.1	100.0	90.1
SFDA-DE [8]	96.0	94.2	76.6	98.5	75.5	99.8	90.1
Source Only	<u>81.9</u>	<u>78.0</u>	<u>59.4</u>	<u>93.6</u>	<u>63.4</u>	<u>98.8</u>	<u>79.2</u>
Ours (w/ ResNet-50)	93.6	90.2	75.8	98.2	72.5	99.2	88.3
Ours (w/ ResNet-101)	94.4	91.6	74.8	98.6	75.6	99.6	89.1
Ours (w/ ConvNext-S)	96.6	92.6	79.8	97.7	79.7	99.4	91.0
Ours (w/ Swin-S)	96.8	93.7	79.4	98.7	<u>80.3</u>	99.6	91.4
Ours (w/ ConvNeXt-B)	97.8	<u>96.7</u>	<u>80.9</u>	98.5	79.5	99.6	<u>92.2</u>
Ours (w/ Swin-B)	<u>97.4</u>	98.2	84.7	<u>99.1</u>	82.2	100.0	93.6

Table 2. Classification accuracy of adapted ResNet-50 for 31-class classification on Office-31. For proposed method, ImageNet-1k feature extractor used in pre-trained model branch is given in parenthesis.

Method	Office-Home												
	A \rightarrow C	A \rightarrow P	A \rightarrow R	C \rightarrow A	C \rightarrow P	C \rightarrow R	P \rightarrow A	P \rightarrow C	P \rightarrow R	R \rightarrow A	R \rightarrow C	R \rightarrow P	Avg
GSDA [13]	<u>61.3</u>	76.1	79.4	65.4	73.3	74.3	65.0	53.2	80.0	72.2	60.6	83.1	70.3
GVB-GD [7]	57.0	74.7	79.8	64.6	74.1	74.6	65.2	55.1	81.0	74.6	59.7	84.3	70.4
RSDA [11]	53.2	77.7	81.3	66.4	74.0	76.5	67.9	53.0	82.0	75.8	57.8	85.4	70.9
TSA [24]	57.6	75.8	80.7	64.3	76.3	75.1	66.7	55.7	81.2	75.7	61.9	83.8	71.2
SRDC [39]	52.3	76.3	81.0	69.5	76.2	78.0	68.7	53.8	81.7	76.3	57.1	85.0	71.3
FixBi [31]	58.1	77.3	80.4	67.7	79.5	78.1	65.8	57.9	81.7	76.4	<u>62.9</u>	86.7	72.7
SFDA [17]	48.4	73.4	76.9	64.3	69.8	71.7	62.7	45.3	76.6	69.8	50.5	79.0	65.7
G-SFDA [45]	57.9	78.6	81.0	66.7	77.2	77.2	65.6	56.0	82.2	72.0	57.8	83.4	71.3
SHOT [26]	57.1	78.1	81.5	68.0	78.2	78.1	67.4	54.9	82.2	73.3	58.8	84.3	71.8
AaD [46]	59.3	79.3	82.1	68.9	79.8	79.5	67.2	57.4	83.1	72.1	58.5	85.4	72.7
A ² Net [42]	58.4	79.0	82.4	67.5	79.3	78.9	68.0	56.2	82.9	74.1	60.5	85.0	72.8
SFDA-DE [8]	59.7	79.5	82.4	69.7	78.6	79.2	66.1	57.2	82.6	73.9	60.8	85.5	72.9
SHOT++ [27]	57.9	79.7	82.5	68.5	79.6	79.3	68.5	57.0	83.0	73.7	60.7	84.9	73.0
Source Only	<u>43.5</u>	<u>67.1</u>	<u>74.2</u>	<u>51.5</u>	<u>62.2</u>	<u>63.3</u>	<u>51.4</u>	<u>40.7</u>	<u>73.2</u>	<u>64.6</u>	<u>45.8</u>	<u>77.6</u>	<u>59.6</u>
Ours (w/ ResNet-50)	51.6	78.9	81.4	66.7	78.9	79.5	66.2	50.1	80.6	71.1	53.7	81.2	70.0
Ours (w/ ResNet-101)	54.6	81.9	83.5	68.6	79.4	80.6	68.6	52.4	82.0	72.2	57.1	84.1	72.1
Ours (w/ ConvNeXt-S)	59.7	<u>86.3</u>	87.2	75.9	84.6	<u>86.8</u>	76.1	58.4	87.1	78.0	61.8	87.1	77.4
Ours (w/ Swin-S)	56.4	85.1	<u>88.0</u>	73.9	83.7	86.2	75.3	55.2	<u>87.9</u>	77.2	58.7	88.0	76.3
Ours (w/ ConvNeXt-B)	60.5	86.2	87.3	<u>76.1</u>	<u>85.4</u>	<u>86.8</u>	<u>76.5</u>	<u>58.5</u>	87.6	<u>79.0</u>	62.5	<u>88.8</u>	<u>77.9</u>
Ours (w/ Swin-B)	69.6	89.6	91.2	82.7	88.5	91.5	82.7	68.8	91.7	82.9	71.4	92.2	83.6

Table 3. Classification accuracy of adapted ResNet-50 for 65-class classification on Office-Home. For proposed method, ImageNet-1k feature extractor used in pre-trained model branch is given in parenthesis.

the best result overall. Co-learning depends on the two branches providing different views of classification decisions. Finetuning the feature extractor or projection layer risks pre-trained model predictions converging too quickly to adaptation model predictions. Additional experiments on NCC computation is provided in Appendix.

Adaptation model branch. On the adaptation model branch, we experiment with other pseudolabeling strategies besides MatchOrConf in Table 6a: SelfConf selects confident samples from adaptation model branch, Other-

Conf selects confident samples from pre-trained model branch, Match selects samples with same predictions on both branches, and MatchAndConf selects confident samples with same predictions on both branches. SelfConf has the worst performance as source model confidence is not well-calibrated on target domain. Overall, MatchOrConf is the best strategy. From Table 6b, the optimal confidence threshold γ differs across datasets. We estimate the ratio of source to ImageNet feature extractor’s target-compatibility using the ratio of average oracle task accuracy on target

Method	VisDA-C												
	plane	bike	bus	car	horse	knife	mcycle	person	plant	sktbrd	train	truck	Avg
SFAN [43]	93.6	61.3	84.1	70.6	94.1	79.0	91.8	79.6	89.9	55.6	89.0	24.4	76.1
MCC [14]	88.7	80.3	80.5	71.5	90.1	93.2	85.0	71.6	89.4	73.8	85.0	36.9	78.8
STAR [30]	95.0	84.0	84.6	73.0	91.6	91.8	85.9	78.4	94.4	84.7	87.0	42.2	82.7
SE [9]	95.9	87.4	85.2	58.6	96.2	95.7	90.6	80.0	94.8	90.8	88.4	47.9	84.3
CAN [15]	97.0	87.2	82.5	74.3	97.8	96.2	90.8	80.7	96.6	<u>96.3</u>	87.5	59.9	87.2
FixBi [31]	96.1	87.8	90.5	90.3	96.8	95.3	92.8	88.7	97.2	94.2	90.9	25.7	87.2
SFDA [17]	86.9	81.7	84.6	63.9	93.1	91.4	86.6	71.9	84.5	58.2	74.5	42.7	76.7
3C-GAN [23]	94.8	73.4	68.8	74.8	93.1	95.4	88.6	84.7	89.1	84.7	83.5	48.1	81.6
SHOT [26]	94.3	88.5	80.1	57.3	93.1	94.9	80.7	80.3	91.5	89.1	86.3	58.2	82.9
A ² Net [42]	94.0	87.8	85.6	66.8	93.7	95.1	85.8	81.2	91.6	88.2	86.5	56.0	84.3
G-SFDA [45]	96.1	88.3	85.5	74.1	97.1	95.4	89.5	79.4	95.4	92.9	89.1	42.6	85.4
SFDA-DE [8]	95.3	91.2	77.5	72.1	95.7	97.8	85.5	<u>86.1</u>	95.5	93.0	86.3	<u>61.6</u>	86.5
SHOT++ [27]	97.7	88.4	<u>90.2</u>	<u>86.3</u>	<u>97.9</u>	98.6	92.9	84.1	<u>97.1</u>	92.2	<u>93.6</u>	28.8	87.3
AaD [46]	97.4	<u>90.5</u>	80.8	76.3	97.3	96.1	89.8	82.9	95.5	93.0	92.0	64.7	88.0
Source Only	51.5	15.3	43.4	75.4	71.2	6.8	85.5	18.8	49.4	46.4	82.1	5.4	45.9
Ours (w/ ResNet-50)	96.0	77.2	77.3	77.4	93.8	96.4	91.4	77.0	90.4	91.3	85.3	50.8	83.7
Ours (w/ ResNet-101)	96.7	78.8	77.3	75.9	95.0	95.7	89.4	77.9	90.5	91.3	85.6	53.1	83.9
Ours (w/ ConvNeXt-S)	97.9	90.1	82.8	81.4	97.1	97.7	93.5	67.7	95.4	96.2	90.7	57.0	87.3
Ours (w/ Swin-S)	97.9	88.6	84.7	78.4	96.8	98.0	93.4	74.4	94.9	94.7	91.2	55.6	87.4
Ours (w/ ConvNeXt-B)	<u>98.1</u>	89.8	85.1	80.1	97.2	<u>98.2</u>	<u>93.8</u>	64.8	95.4	96.4	90.5	55.2	87.0
Ours (w/ Swin-B)	99.1	90.4	84.3	80.9	98.1	98.1	95.3	80.5	94.9	95.9	94.7	48.6	88.4

Table 4. Classification accuracy of adapted ResNet-101 for 12-class classification on VisDA-C. For proposed method, ImageNet-1k feature extractor used in pre-trained model branch is given in parenthesis.

Feat. extr.	Classifier	Projection	A → C	A → P	A → R	Avg
✗	✗	✗	59.4	83.8	86.5	76.6
✓	✗	✗	59.6	82.6	86.4	76.2
✓	✓	✗	60.3	84.9	86.4	77.2
✗	✓	✗	<u>59.7</u>	86.3	<u>87.1</u>	77.7
✗	✓	✓	59.5	<u>85.9</u>	87.2	<u>77.5</u>
✗	✗	✓	59.5	84.1	86.5	76.7

Table 5. Co-learning experiments on the component finetuned in pre-trained model branch on Office-Home, with ImageNet-1k ConvNeXt-S in pre-trained model branch.

domains, computed by fitting a nearest-centroid-classifier head using fully-labeled target samples for each of the two feature extractors. When the ratio is low as in VisDA-C, the ImageNet feature extractor is more target-compatible, and lowering γ allows it to pseudolabel more samples according to its predictions. We include per-domain oracle task accuracy values in the Appendix.

Training curves. Figure 4 visualizes the co-learning process for VisDA-C. The proportion of target pseudolabels increases from 0.542 to 0.925 over 15 episodes. Classification accuracy on pre-trained model branch starts higher as the ImageNet feature extractor is more target-compatible than source feature extractor, and flattens earlier since its features are fixed. The adaptation model learns from pre-trained model predictions, and surpasses its accuracy as the feature extractor continues to adapt.

5.2. Prediction sharpening

In Table 7, for each dataset, prediction sharpening adds up to 0.2% to model performance. We note that most of

Pseudolabel strategy	A → C	A → P	A → R	Avg
SelfConf	49.1	74.8	77.1	67.0
OtherConf	57.5	<u>85.4</u>	<u>86.7</u>	76.5
Match	61.3	84.2	86.0	<u>77.2</u>
MatchOrConf	59.7	86.3	87.1	77.7
MatchAndConf	<u>60.3</u>	81.3	84.5	75.4

(a) Pseudolabeling strategies, on Office-Home

Confidence threshold γ	Office-31	Office-Home	VisDA
0.1	90.5	76.1	87.1
0.3	91.2	77.1	<u>86.8</u>
0.5	<u>91.0</u>	77.4	86.4
0.7	90.8	77.5	85.8
0.9	90.8	77.3	85.5
Target-compatibility ratio	0.982	0.947	0.844

(b) Confidence threshold in MatchOrConf pseudolabeling strategy. Target-compatibility ratio estimated by ratio of source to pre-trained model’s average oracle task accuracy on target domains.

Table 6. Co-learning experiments on the adaptation model branch, with ImageNet-1k ConvNeXt-S in pre-trained model branch.

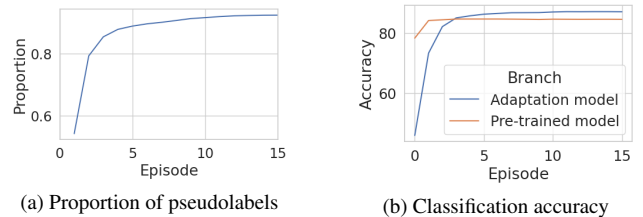


Figure 4. VisDA-C co-learning training curves, with ImageNet-1k ConvNeXt-S in pre-trained model branch..

the performance improvement in our proposed method is attributed to co-learning, and the effect of prediction sharp-

Pre-trained feat. extr.	Office-31		Office-Home		VisDA-C	
	Co-learn	Full	Co-learn	Full	Co-learn	Full
ResNet-50	88.3	88.3	70.0	70.0	83.5	83.7 (↑)
ResNet-101	89.0	89.1 (↑)	72.1	72.1	83.7	83.9 (↑)
ConvNeXt-S	91.0	91.0	77.4	77.4	87.1	87.3 (↑)
Swin-S	91.3	91.4 (↑)	76.3	76.3	87.2	87.4 (↑)
ConvNeXt-B	92.1	92.2 (↑)	77.9	77.9	86.8	87.0 (↑)
Swin-B	93.6	93.6	83.5	83.6 (↑)	88.2	88.4 (↑)

Table 7. Ablation study for prediction sharpening. ‘Full’ denotes further prediction sharpening after co-learning.

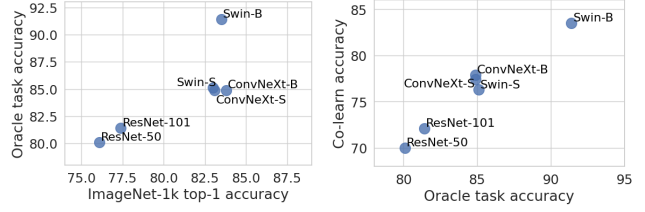
ening is expected to be larger when the quantity of non-pseudolabeled samples is higher. For VisDA-C truck class, prediction sharpening increases accuracy by 0.5% to 1.9% for all feature extractors tested. We refer readers to the Appendix for full results.

5.3. Discussion

We further explore considerations on the characteristics of the pre-trained feature extractor used for co-learning and the effectiveness of our proposed method.

What are preferred characteristics of the feature extractor for co-learning? We first study this in Figure 5 through the relationship of ImageNet-1k top-1 accuracy and Office-Home average target domain accuracy. In general, a feature extractor with higher ImageNet accuracy has learned better representations and hence has higher oracle accuracy on target domain, and consequently helps to better adapt the source model through co-learning. Next, we study a few specific source-domain pairs in Table 8 by plugging source and ImageNet-1k feature extractors into the pre-trained model branch, and observe effects of the following positive characteristics: (1) Dataset similarity (style and task): In $C \rightarrow R$ with the same ResNet-50 architecture, there are ImageNet samples more similar to Real World target than Clipart source is, as ImageNet-1k ResNet-50 has higher oracle accuracy than Source ResNet-50. (2) Better architectures: In $A \rightarrow C$ with ResNet-50, although ImageNet is less similar to Clipart target than Art source is, changing to ResNet-101 learns better representations and improves oracle accuracy. (3) Different views: In $R \rightarrow A$, although ImageNet-1k ResNet-50 has slightly worse oracle accuracy than Source ResNet-50 (81.2% vs. 81.8%), co-learning with it has better adaptation performance (71.1% vs. 70.5%). Since the adaptation model branch is already initialized by source model, using ImageNet feature extractor in the other branch provides a different view of features and consequently classification decision which benefits co-learning. We refer readers to the Appendix for the full comparison of ResNets on all 3 datasets.

Since modern ImageNet feature extractors have learned better representations, is it sufficient to use them in source models and not adapt? In Table 9, we fit a 2-layer linear classification head as in Section 4.1 on ImageNet-1k ConvNext-B and Swin-B feature extractors by accessing



(a) Oracle task accuracy versus ImageNet-1k top-1 accuracy (b) Classification accuracy after co-learning versus oracle task accuracy

Figure 5. Performance evaluations of ImageNet-1k feature extractors. Average oracle task accuracy of ImageNet-1k feature extractor, and average classification accuracy of adapted model co-learned with ImageNet-1k feature extractor, are evaluated on Office-Home target domains.

Pre-trained feat. extr.	C \rightarrow R		A \rightarrow C		R \rightarrow A	
	Oracle	Co-learn	Oracle	Co-learn	Oracle	Co-learn
Source ResNet-50	83.3	74.1	69.5	<u>53.9</u>	<u>81.8</u>	70.5
ImageNet-1k ResNet-50	<u>86.0</u>	<u>79.4</u>	65.5	51.8	81.2	<u>71.1</u>
ImageNet-1k ResNet-101	87.0	80.4	<u>68.0</u>	54.6	82.5	72.4

Table 8. Oracle task accuracy of pre-trained feature extractor on target domain, and classification accuracy of adapted model co-learned with pre-trained feature extractor, on Office-Home.

Model	A \rightarrow C	A \rightarrow P	A \rightarrow R	Avg
ConvNext-B + classification head [†]	56.1	78.6	83.3	72.7
ResNet-50 adapted w/ ConvNeXt-B	60.5	86.2	87.3	78.0
Swin-B + classification head [†]	67.1	86.7	89.1	81.0
ResNet-50 adapted w/ Swin-B	69.6	89.6	91.2	83.5

Table 9. Comparison of classification accuracy of ImageNet-1k feature extractor fitted with source-trained classification head, versus classification accuracy of adapted ResNet-50, on Office-Home. [†] denotes classifier is trained on fully-labeled source data.

and training the classifier on fully-labeled source data. On the set of Office-Home domain pairs tested, average performance of Swin-B + classification head is 8.3% higher than ConvNext-B + classification head, showing that feature extractor choice can indeed reduce negative effects of domain shift. However, adaptation to target domain is still necessary. Without having to access the source data and using a larger source model, our proposed source-free DA approach achieves higher classification accuracy.

6. Conclusion

In this work, we proposed a new methodology for source-free domain adaptation that utilizes an ImageNet pre-trained feature extractor to improve target pseudolabel quality to finetune the source model. This framework allows us to leverage modern publicly available pre-trained networks that may be more compatible with the target domain. Experiments on benchmark datasets demonstrate the effectiveness of our approach.

Acknowledgments

This research is supported by the Agency for Science, Technology and Research (A*STAR) under its AME Programmatic Funds (Grant No. A20H6b0151).

References

- [1] Hugging Face - models. <https://huggingface.co/models>. 3
- [2] PyTorch - models and pre-trained weights. <https://pytorch.org/vision/stable/models.html>. 3
- [3] TensorFlow - models and datasets. <https://www.tensorflow.org/resources/models-datasets>. 3
- [4] S. Ben-David, J. Blitzer, K. Crammer, A. Kulesza, F. Pereira, and J.W. Vaughan. A theory of learning from different domains. *Machine Learning*, 79(1):151–175, 2010. 1, 3
- [5] J. Blitzer, K. Crammer, A. Kulesza, F. Pereira, and J. Wortman. Learning bounds for domain adaptation. In *NeurIPS*, 2007. 3
- [6] W. Chen, L. Lin, S. Yang, D. Xie, S. Pu, Y. Zhuang, and W. Ren. Self-supervised noisy label learning for source-free unsupervised domain adaptation. *ArXiv*, 2021. 1, 3
- [7] S. Cui, S. Wang, J. Zhuo, C. Su, Q. Huang, and Q. Tian. Gradually vanishing bridge for adversarial domain adaptation. In *CVPR*, 2020. 3, 6
- [8] N. Ding, Y. Xu, Y. Tang, Y. Wang, and D. Tao. Source-free domain adaptation via distribution estimation. *CVPR*, 2022. 1, 3, 6, 7
- [9] G. French, M. Mackiewicz, and M. Fisher. Self-ensembling for domain adaptation. In *ICLR*, 2018. 3, 7
- [10] Y. Ganin, E. Ustinova, H. Ajakan, P. Germain, H. Larochelle, F. Laviolette, M. Marchand, and V. Lempitsky. Domain-adversarial training of neural networks. *Journal of Machine Learning Research*, 17:59:1–59:35, 2016. 1, 3
- [11] X. Gu, J. Sun, and Z. Xu. Spherical space domain adaptation with robust pseudo-label loss. In *CVPR*, 2020. 1, 3, 6
- [12] I. Gulrajani and D. Lopez-Paz. In search of lost domain generalization. *ICLR*, 2021. 1
- [13] L. Hu, M. Kan, S. Shan, and X. Chen. Unsupervised domain adaptation with hierarchical gradient synchronization. In *CVPR*, 2020. 1, 3, 6
- [14] Y. Jin, X. Wang, M. Long, and J. Wang. Minimum class confusion for versatile domain adaptation. In *ECCV*, 2020. 3, 6, 7
- [15] G. Kang, L. Jiang, Y. Yang, and A. Hauptmann. Contrastive adaptation network for unsupervised domain adaptation. *CVPR*, 2019. 1, 3, 6, 7
- [16] D. Kim, K. Wang, S. Sclaroff, and K. Saenko. A broad study of pre-training for domain generalization and adaptation. *ArXiv*, 2022. 5
- [17] Y. Kim, D. Cho, K. Han, P. Panda, and S. Hong. Domain adaptation without source data. *IEEE Transactions on Artificial Intelligence*, 2(6):508–518, 2021. 1, 3, 6, 7
- [18] P. Koh, S. Sagawa, H. Marklund, S. Xie, M. Zhang, A. Balsubramani, W. Hu, M. Yasunaga, R. Phillips, S. Beery, J. Leskovec, A. Kundaje, E. Pierson, S. Levine, C. Finn, and P. Liang. Wilds: A benchmark of in-the-wild distribution shifts. *ArXiv*, 2020. 1
- [19] J. N. Kundu, S. Bhambri, A. Kulkarni, H. Sarkar, V. Jampani, and R. V. Babu. Concurrent subsidiary supervision for unsupervised source-free domain adaptation. In *ECCV*, 2022. 3
- [20] J. N. Kundu, A. Kulkarni, S. Bhambri, D. Mehta, S. Kulkarni, V. Jampani, and R. V. Babu. Balancing discriminability and transferability for source-free domain adaptation. In *ICML*, 2022. 3
- [21] J. N. Kundu, N. Venkat, R. Ambareesh, R. M. V., and R. V. Babu. Towards inheritable models for open-set domain adaptation. *CVPR*, 2020. 1, 3
- [22] H. Li, S. J. Pan, S. Wang, and A. C. Kot. Domain generalization with adversarial feature learning. *CVPR*, 2018. 1, 3
- [23] R. Li, Q. Jiao, W. Cao, H.-S. Wong, and S. Wu. Model adaptation: Unsupervised domain adaptation without source data. *CVPR*, 2020. 1, 3, 6, 7
- [24] S. Li, M. Xie, K. Gong, Chi H. Liu, Y. Wang, and W. Li. Transferable semantic augmentation for domain adaptation. In *CVPR*, 2021. 3, 6
- [25] Y. Li, X. Tian, M. Gong, Y. Liu, T. Liu, K. Zhang, and D. Tao. Deep domain generalization via conditional invariant adversarial networks. *ECCV*, 2018. 1, 3
- [26] J. Liang, D. Hu, and J. Feng. Do we really need to access the source data? source hypothesis transfer for unsupervised domain adaptation. *ICML*, 2020. 1, 3, 4, 5, 6, 7
- [27] J. Liang, D. Hu, Y. Wang, R. He, and J. Feng. Source data-absent unsupervised domain adaptation through hypothesis transfer and labeling transfer. *IEEE TPAMI*, 2021. 1, 3, 5, 6, 7
- [28] Z. Liu, Y. Lin, Y. Cao, H. Hu, Y. Wei, Z. Zhang, S. Lin, and B. Guo. Swin transformer: Hierarchical vision transformer using shifted windows. In *ICCV*, 2021. 2, 5
- [29] Z. Liu, H. Mao, CY. Wu, C. Feichtenhofer, T. Darrell, and S. Xie. A convnet for the 2020s. *CVPR*, 2022. 5
- [30] Z. Lu, Y. Yang, X. Zhu, C. Liu, YZ. Song, and T. Xiang. Stochastic classifiers for unsupervised domain adaptation. In *CVPR*, 2020. 3, 7
- [31] J. Na, H. Jung, H. J. Chang, and W. Hwang. Fixbi: Bridging domain spaces for unsupervised domain adaptation. In *CVPR*, 2021. 3, 6, 7
- [32] Y. Ovadia, E. Fertig, J. Ren, Z. Nado, D. Sculley, S. Nowozin, J. Dillon, B. Lakshminarayanan, and J. Snoek. Can you trust your model's uncertainty? evaluating predictive uncertainty under dataset shift. In *NeurIPS*, 2019. 1
- [33] X. Peng, B. Usman, N. Kaushik, J. Hoffman, D. Wang, and Kate Saenko. Visda: The visual domain adaptation challenge. *ArXiv*, abs/1710.06924, 2017. 5
- [34] Z. Qiu, Y. Zhang, H. Lin, S. Niu, Y. Liu, Q. Du, and M. Tan. Source-free domain adaptation via avatar prototype generation and adaptation. *IJCAI*, 2021. 1, 3
- [35] S. Qu, G. Chen, J. Zhang, Z. Li, W. He, and D. Tao. BMD: A general class-balanced multicentric dynamic prototype strategy for source-free domain adaptation. In *ECCV*, 2022. 3
- [36] S. Roy, M. Trapp, A. Pilzer, J. Kannala, N. Sebe, E. Ricci, and A. Solin. Uncertainty-guided source-free domain adaptation. In *ECCV*, 2022. 3

- [37] K. Saenko, B. Kulis, M. Fritz, and T. Darrell. Adapting visual category models to new domains. *ECCV*, 2010. 5
- [38] B. Sun and K. Saenko. Deep coral: Correlation alignment for deep domain adaptation. *ECCV Workshops*, 2016. 1, 3
- [39] H. Tang, K. Chen, and K. Jia. Unsupervised domain adaptation via structurally regularized deep clustering. In *CVPR*, 2020. 3, 6
- [40] Hemanth Venkateswara, Jose Eusebio, Shayok Chakraborty, and Sethuraman Panchanathan. Deep hashing network for unsupervised domain adaptation. *CVPR*, 2017. 5
- [41] G. Wilson and D. J. Cook. A survey of unsupervised deep domain adaptation. *ACM Trans. Intell. Syst. Technol.*, 11(5), July 2020. 1, 3
- [42] H. Xia, H. Zhao, and Z. Ding. Adaptive adversarial network for source-free domain adaptation. *ICCV*, 2021. 1, 3, 6, 7
- [43] R. Xu, G. Li, J. Yang, and L. Lin. Larger norm more transferable: An adaptive feature norm approach for unsupervised domain adaptation. In *ICCV*, 2019. 1, 3, 7
- [44] S. Yang, Y. Wang, J. van de Weijer, L. Herranz, and S. Jui. Exploiting the intrinsic neighborhood structure for source-free domain adaptation. In *NeurIPS*, 2021. 1, 3
- [45] S. Yang, Y. Wang, J. van de Weijer, L. Herranz, and S. Jui. Generalized source-free domain adaptation. In *ICCV*, 2021. 1, 3, 6, 7
- [46] S. Yang, Y. Wang, K. Wang, S. Jui, and J. van de Weijer. Attracting and dispersing: A simple approach for source-free domain adaptation. *NeurIPS*, 2022. 1, 3, 6, 7
- [47] Y. Zhang, T. Liu, M. Long, and M. Jordan. Bridging theory and algorithm for domain adaptation. In *ICML*, 2019. 1, 3, 6

Centroid computation	A \rightarrow C	A \rightarrow P	A \rightarrow R	Avg
All samples	59.7	86.3	87.1	77.7
Partial samples	59.1	86.1	87.0	77.4

(a) Samples used to estimate class centroids in classifier: all samples versus only samples pseudolabeled by MatchOrConf

# Iterations	A \rightarrow C	A \rightarrow P	A \rightarrow R	Avg
1	59.7	86.3	87.1	77.7
2	58.2	85.5	87.2	77.0
3	57.7	85.9	86.6	76.7

(b) Number of iterations to estimate class centroids in classifier

Table 10. Co-learning experiments on the weighted nearest-centroid classifier in pre-trained model branch on Office-Home, with ImageNet-1k ConvNeXt-S in pre-trained model branch.

Appendix

A. Detailed Results

We provide detailed results of experiments to analyze our proposed method.

A.1. Co-learning

Pre-trained model branch. We experiment with the computation of weighted nearest-centroid-classifier (NCC) in the pre-trained model branch in Table 10. In Table 10a, we find that class centroids in the NCC classifier should be estimated using all samples, instead of only pseudolabeled samples, to better represent the entire target data distribution. Table 10b shows that refining class centroids iteratively (as in k-means) is not beneficial, as the model predictions used for centroid estimation have inaccuracies and increased iterations can reinforce the bias that these inaccuracies have on the resulting centroids.

A.2. Prediction sharpening

In Table 11a, 11b and 11c, we provide detailed results of our proposed method for the 3 benchmark datasets Office-31, Office-Home and VisDA-C. Apart from the full adapted model performance (after co-learning and prediction sharpening) presented in the main manuscript, we include intermediate model performance after co-learning. We note that most of the performance improvement in our proposed method is attributed to co-learning. Prediction sharpening adds up to 0.4% per-domain accuracy in Office-31, 0.3% per-domain accuracy in Office-Home, and 1.9% per-class accuracy in VisDA-C.

Since prediction sharpening performs entropy minimization on non-pseudolabeled samples after the co-learning stage, its effect is expected to be larger when the quantity of non-pseudolabeled samples is higher. Figure 6 plots the proportion of pseudolabeled samples on target domains after co-learning with different pre-trained feature extractors. Overall, the percentage of samples pseudolabeled is

96.4% to 100% in Office-31, 91.8% to 98.7% in Office-Home with percentage above 94% in most cases, and 90.5% to 92.5% in VisDA-C. Due to the greater proportion of non-pseudolabeled samples in VisDA-C, prediction sharpening can have a larger effect. For the VisDA-C truck class, prediction sharpening increases accuracy by 0.5% to 1.9% for all pre-trained feature extractors tested.

A.3. Characteristics of pre-trained feature extractor

We provide detailed results on the study of preferred feature extractor characteristics for co-learning.

Target domain oracle accuracy versus ImageNet-1k accuracy. We plot the relationship of ImageNet-1k top-1 accuracy and average target domain oracle task accuracy attained by pre-trained feature extractors for each dataset in Figure 7, and list the per-domain values in Table 12. Oracle task accuracy is computed by fitting a nearest-centroid-classifier head on each pre-trained feature extractor using fully-labeled target data. In general, higher ImageNet-1k top-1 accuracy corresponds to higher target domain oracle accuracy. However, there are exceptions. For instance, Swin-B has lower ImageNet-1k accuracy than ConvNext-B (83.5% vs. 83.8%), but higher oracle accuracy for all target domains tested. Despite being trained on the same ImageNet-1k and achieving similar ImageNet-1k performance, the feature extractors learn different features due to differences in architecture and training schemes, and the Swin-B features may be more robust to distribution shift and more compatible with the target domains tested.

Adapted model accuracy versus target domain oracle accuracy We also plot the relationship of average oracle task accuracy of pre-trained feature extractors and the performance of adapted model after co-learning on target domains in Figure 7. In general, a pre-trained feature extractor with higher oracle task accuracy benefits co-learning as it is more capable of correctly pseudolabeling the target samples, and consequently results in higher adapted model performance. For instance in Table 13, by using ResNet architectures for co-learning in the pre-trained model branch, we see that the larger and more powerful ImageNet-1k ResNet-101 typically results in higher adapted model performance than ImageNet-1k ResNet-50. There are also exceptions to this correlation. With the same ResNet-50 architecture, although source ResNet-50 has higher oracle accuracy than ImageNet-1k ResNet-50 in some source-target domain pairs (e.g. Office-31 $A \rightarrow D$, $A \rightarrow W$, $W \rightarrow D$; Office-Home $A \rightarrow R$, $P \rightarrow C$, $R \rightarrow A$), the latter results in equal or higher adapted model performance. The ImageNet feature extractors benefit co-learning as they provide an additional view of features and classification decisions different from the source feature extractor already in the adaptation model branch.

Method	Office-31						
	A \rightarrow D	A \rightarrow W	D \rightarrow A	D \rightarrow W	W \rightarrow A	W \rightarrow D	Avg
Source Only	81.9	78.0	59.4	93.6	63.4	98.8	79.2
Co-learn (w/ Resnet-50)	93.6	90.2	75.7	98.2	72.5	99.4	88.3
+ Prediction sharpening	93.6	90.2	75.8	98.2	72.5	99.2	88.3
Co-learn (w/ Resnet-101)	94.2	91.6	74.7	98.6	75.6	99.6	89.0
+ Prediction sharpening	94.4	91.6	74.8	98.6	75.6	99.6	89.1
Co-learn (w/ ConvNeXt-S)	96.6	92.6	79.8	97.7	79.6	99.4	91.0
+ Prediction sharpening	96.6	92.6	79.8	97.7	79.7	99.4	91.0
Co-learn (w/ Swin-S)	96.8	93.3	79.2	98.7	80.2	99.6	91.3
+ Prediction sharpening	96.8	93.7	79.4	98.7	80.3	99.6	91.4
Co-learn (w/ ConvNeXt-B)	97.8	96.6	80.5	98.5	79.4	99.6	92.1
+ Prediction sharpening	97.8	96.7	80.9	98.5	79.5	99.6	92.2
Co-learn (w/ Swin-B)	97.4	98.2	84.5	99.1	82.2	100.0	93.6
+ Prediction sharpening	97.4	98.2	84.7	99.1	82.2	100.0	93.6

(a) Classification accuracy of adapted ResNet-50 for 31-class classification on Office-31

Method	Office-Home												
	A \rightarrow C	A \rightarrow P	A \rightarrow R	C \rightarrow A	C \rightarrow P	C \rightarrow R	P \rightarrow A	P \rightarrow C	P \rightarrow R	R \rightarrow A	R \rightarrow C	R \rightarrow P	Avg
Source Only	43.5	67.1	74.2	51.5	62.2	63.3	51.4	40.7	73.2	64.6	45.8	77.6	59.6
Co-learn (w/ Resnet-50)	51.8	78.9	81.3	66.7	78.8	79.4	66.3	50.0	80.6	71.1	53.7	81.3	70.0
+ Prediction sharpening	51.6	78.9	81.4	66.7	78.9	79.5	66.2	50.1	80.6	71.1	53.7	81.2	70.0
Co-learn (w/ Resnet-101)	54.6	81.8	83.5	68.6	79.3	80.4	68.7	52.3	82.0	72.4	57.1	84.1	72.1
+ Prediction sharpening	54.6	81.9	83.5	68.6	79.4	80.6	68.6	52.4	82.0	72.2	57.1	84.1	72.1
Co-learn (w/ ConvNeXt-S)	59.7	86.3	87.1	75.9	84.5	86.8	76.1	58.7	87.1	78.0	61.9	87.2	77.4
+ Prediction sharpening	59.7	86.3	87.2	75.9	84.6	86.8	76.1	58.4	87.1	78.0	61.8	87.1	77.4
Co-learn (w/ Swin-S)	56.4	85.1	88.0	73.9	83.7	86.1	75.4	55.3	87.8	77.3	58.9	87.9	76.3
+ Prediction sharpening	56.4	85.1	88.0	73.9	83.7	86.2	75.3	55.2	87.9	77.2	58.7	88.0	76.3
Co-learn (w/ ConvNeXt-B)	60.5	85.9	87.2	76.1	85.3	86.6	76.5	58.6	87.5	78.9	62.4	88.8	77.9
+ Prediction sharpening	60.5	86.2	87.3	76.1	85.4	86.8	76.5	58.5	87.6	79.0	62.5	88.8	77.9
Ours (w/ Swin-B)	69.6	89.5	91.2	82.7	88.4	91.3	82.6	68.5	91.5	82.8	71.3	92.1	83.5
+ Prediction sharpening	69.6	89.6	91.2	82.7	88.5	91.5	82.7	68.8	91.7	82.9	71.4	92.2	83.6

(b) Classification accuracy of adapted ResNet-50 for 65-class classification on Office-Home

Method	VisDA-C												
	plane	bike	bus	car	horse	knife	mcycle	person	plant	sktbrd	train	truck	Avg
Source Only	51.5	15.3	43.4	75.4	71.2	6.8	85.5	18.8	49.4	46.4	82.1	5.4	45.9
Co-learn (w/ Resnet-50)	96.2	76.2	77.5	77.8	93.8	96.6	91.5	76.7	90.4	90.8	86.0	48.9	83.5
+ Prediction sharpening	96.0	77.2	77.3	77.4	93.8	96.4	91.4	77.0	90.4	91.3	85.3	50.8	83.7
Co-learn (w/ Resnet-101)	96.5	78.9	77.5	75.7	94.6	95.8	89.1	77.7	90.5	91.0	86.2	51.5	83.7
+ Prediction sharpening	96.7	78.8	77.3	75.9	95.0	95.7	89.4	77.9	90.5	91.3	85.6	53.1	83.9
Co-learn (w/ ConvNeXt-S)	97.8	89.7	82.3	81.3	97.3	97.8	93.4	66.9	95.4	96.0	90.7	56.5	87.1
+ Prediction sharpening	97.9	90.1	82.8	81.4	97.1	97.7	93.5	67.7	95.4	96.2	90.7	57.0	87.3
Co-learn (w/ Swin-S)	97.8	88.5	84.7	78.5	96.8	97.8	93.3	73.9	94.9	94.8	91.2	54.8	87.2
+ Prediction sharpening	97.9	88.6	84.7	78.4	96.8	98.0	93.4	74.4	94.9	94.7	91.2	55.6	87.4
Co-learn (w/ ConvNeXt-B)	98.0	89.2	84.9	80.2	97.0	98.4	93.6	64.3	95.6	96.3	90.4	54.0	86.8
+ Prediction sharpening	98.1	89.8	85.1	80.1	97.2	98.2	93.8	64.8	95.4	96.4	90.5	55.2	87.0
Co-learn (w/ Swin-B)	99.0	90.0	84.2	81.0	98.1	97.9	94.9	80.1	94.8	95.9	94.4	48.1	88.2
+ Prediction sharpening	99.1	90.4	84.3	80.9	98.1	98.1	95.3	80.5	94.9	95.9	94.7	48.6	88.4

(c) Classification accuracy of adapted ResNet-101 for 12-class classification on VisDA-C

Table 11. Classification accuracy of adapted models. For proposed method, ImageNet-1k feature extractor used in pre-trained model branch is given in parenthesis.

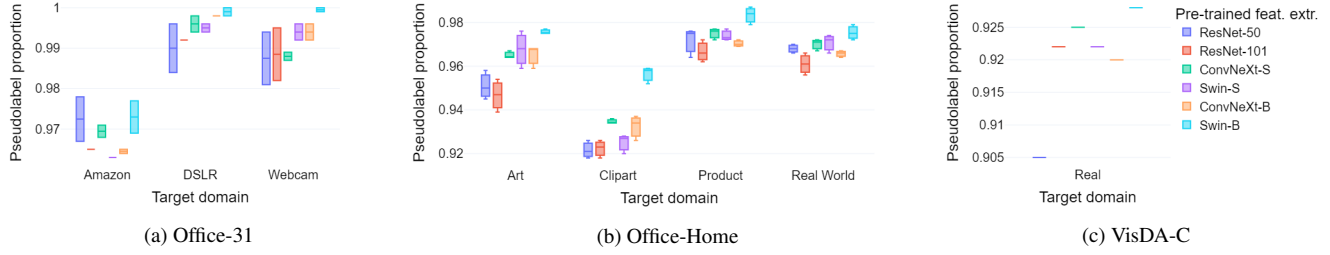


Figure 6. Proportion of pseudolabeled samples after co-learning with ImageNet-1k pre-trained feature extractor.

Pre-training data	Feat. extr.	# Param.	IN-1k Acc@1	Office-31			
				Amazon	DSLIR	Webcam	Avg
ImageNet-1k, then Amazon	ResNet-50	26M	-	-	98.6	98.1	-
ImageNet-1k, then DSLIR	ResNet-50	26M	-	80.1	-	97.7	-
ImageNet-1k, then Webcam	ResNet-50	26M	-	81.7	99.2	-	-
ImageNet-1k	ResNet-50	26M	76.1	81.8	98.2	97.9	92.6
ImageNet-1k	ResNet-101	45M	77.4	83.4	98.8	97.9	93.4
ImageNet-1k	ConvNeXt-S	50M	83.1	85.2	99.4	98.2	94.3
ImageNet-1k	Swin-S	50M	83.0	86.2	99.0	99.4	94.9
ImageNet-1k	ConvNeXt-B	89M	83.8	86.2	99.4	98.6	94.7
ImageNet-1k	Swin-B	88M	83.5	90.6	100.0	100.0	96.9

(a) Target domain oracle task accuracy of pre-trained feature extractors on Office-31

Pre-training data	Feat. extr.	# Param.	IN-1k Acc@1	Office-Home				
				Art	Clipart	Product	Real World	Avg
ImageNet-1k, then Art	ResNet-50	26M	-	-	69.5	88.1	86.3	-
ImageNet-1k, then Clipart	ResNet-50	26M	-	79.3	-	86.0	83.3	-
ImageNet-1k, then Product	ResNet-50	26M	-	80.0	67.5	-	85.8	-
ImageNet-1k, then Real World	ResNet-50	26M	-	81.8	69.1	88.1	-	-
ImageNet-1k	ResNet-50	26M	76.1	81.2	65.5	87.7	86.0	80.1
ImageNet-1k	ResNet-101	45M	77.4	82.5	68.0	88.2	87.0	81.4
ImageNet-1k	ConvNeXt-S	50M	83.1	86.0	72.3	91.7	89.4	84.9
ImageNet-1k	Swin-S	50M	83.0	86.6	72.0	91.5	90.2	85.1
ImageNet-1k	ConvNeXt-B	89M	83.8	85.7	73.4	91.4	89.2	84.9
ImageNet-1k	Swin-B	88M	83.5	92.3	83.1	95.3	94.7	91.4

(b) Target domain oracle task accuracy of pre-trained feature extractors on Office-Home

Pre-training data	Feat. extr.	# Param.	IN-1k Acc@1	VisDA-C
ImageNet-1k, then Synthetic	ResNet-101	45M	-	71.6
ImageNet-1k	ResNet-50	26M	76.1	80.7
ImageNet-1k	ResNet-101	45M	77.4	81.5
ImageNet-1k	ConvNeXt-S	50M	83.1	84.8
ImageNet-1k	Swin-S	50M	83.0	84.9
ImageNet-1k	ConvNeXt-B	89M	83.8	85.0
ImageNet-1k	Swin-B	88M	83.5	86.3

(c) Target domain oracle task accuracy of pre-trained feature extractors on VisDA-C

Table 12. Target domain oracle task accuracy of pre-trained feature extractors fitted with nearest-centroid-classifier heads learned on fully-labeled target domain data. IN-1k Acc@1 denotes ImageNet-1k top-1 accuracy. Feature extractors above dash line are from source models, below the dash line are from ImageNet-1k networks.

Pre-trained feat. extr.	Office-31						
	A \rightarrow D	A \rightarrow W	D \rightarrow A	D \rightarrow W	W \rightarrow A	W \rightarrow D	Avg
Source ResNet-50	92.6	89.9	74.0	96.1	<u>73.9</u>	<u>99.4</u>	87.6
ImageNet-1k ResNet-50	<u>93.6</u>	<u>90.2</u>	75.7	<u>98.2</u>	72.5	<u>99.4</u>	<u>88.3</u>
ImageNet-1k ResNet-101	94.2	91.6	<u>74.7</u>	98.6	75.6	99.6	89.0

(a) Classification accuracy of adapted ResNet-50 on Office-31

Pre-trained feat. extr.	Office-Home												
	A \rightarrow C	A \rightarrow P	A \rightarrow R	C \rightarrow A	C \rightarrow P	C \rightarrow R	P \rightarrow A	P \rightarrow C	P \rightarrow R	R \rightarrow A	R \rightarrow C	R \rightarrow P	Avg
Source ResNet-50	53.9	79.0	81.3	63.5	75.6	74.1	63.7	49.8	80.1	70.5	54.8	81.4	69.0
ImageNet-1k ResNet-50	51.8	78.9	81.3	66.7	78.8	79.4	66.3	50.0	80.6	71.1	53.7	81.3	70.0
ImageNet-1k ResNet-101	54.6	81.8	83.5	68.6	79.3	80.4	68.7	52.3	82.0	72.4	57.1	84.1	72.1

(b) Classification accuracy of adapted ResNet-50 on Office-Home

Pre-trained feat. extr.	VisDA-C												
	plane	bike	bus	car	horse	knife	mcycle	person	plant	sktbrd	train	truck	Avg
Source ResNet-101	63.6	55.6	<u>68.0</u>	65.6	84.0	95.6	89.0	65.8	82.6	4.9	82.2	25.8	65.2
ImageNet-1k ResNet-50	<u>96.2</u>	<u>76.2</u>	77.5	77.8	<u>93.8</u>	96.6	91.5	<u>76.7</u>	<u>90.4</u>	<u>90.8</u>	<u>86.0</u>	<u>48.9</u>	<u>83.5</u>
ImageNet-1k ResNet-101	96.5	78.9	77.5	<u>75.7</u>	94.6	<u>95.8</u>	<u>89.1</u>	77.7	90.5	91.0	86.2	51.5	83.7

(c) Classification accuracy of adapted ResNet-101 on VisDA-C

Table 13. Classification accuracy of adapted model, after co-learning with ResNets in pre-trained model branch.

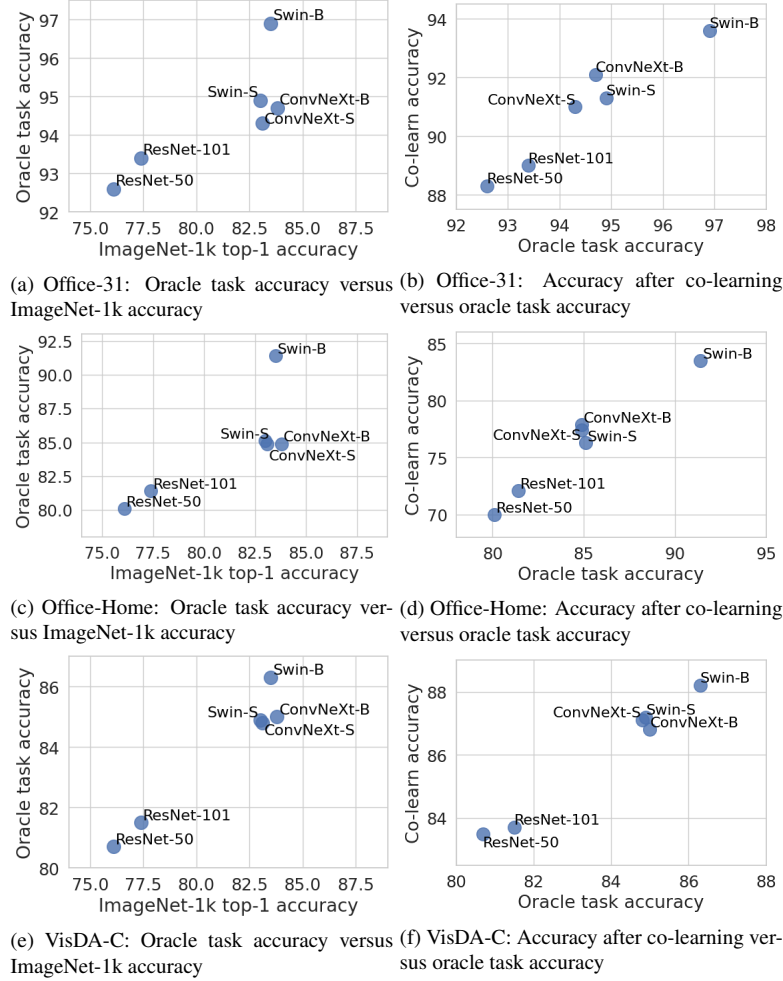


Figure 7. Performance evaluations of ImageNet-1k feature extractors. Average oracle task accuracy of ImageNet-1k feature extractor, and average classification accuracy of adapted model co-learned with ImageNet-1k feature extractor, are evaluated on dataset target domains.